Materials and Design 53 (2014) 915–920

Contents lists available at ScienceDirect

Materials and Design

journal homepage: www.elsevier.com/locate/matdes

Dissimilar pulsed Nd:YAG laser welding of pure niobium to Ti–6Al–4V

M.J. Torkamany, F. Malek Ghaini *, R. Poursalehi

Department of Materials Engineering, Tarbiat Modares University, P.O. Box 14115-143, Tehran, Iran

ARTICLE INFO

Article history:
Received 16 May 2013
Accepted 29 July 2013
Available online 6 August 2013

Keywords:
Ti–6Al–4V
Pure niobium
Laser welding
Pulsed Nd:YAG laser

ABSTRACT

Dissimilar butt welding of pure niobium plate to the titanium alloy Ti–6Al–4V sheet using a pulsed Nd:YAG laser is performed. Effects of laser pulse energy, duration and repetition rates on the melt profile on both sides of the weld line were investigated. Considering the thermo-physical properties of the two base metals, variation of the weld profiles on different sides of the weld line is discussed. Through optimization of the process parameters a sound weld with full penetration along the dissimilar interface was obtained. However, islands of Ti rich and Nb rich phases were identified in the weld metal. Tensile strength of the welded joints matched that of the weaker base metal i.e. niobium and the specimens broke outside the fusion line.

1. Introduction

Titanium alloy Ti–6Al–4V has been widely used in high performance structures because of its high level of strength to weight ratio and superior corrosion resistance. Niobium is a refractory metal having superior superconducting properties. The critical temperature of niobium is higher than other metals and becomes superconductor at 9 K which is just above the liquid helium temperature (4 K) [1]. Superconducting radio frequency (SRF) cavities are widely used for particle accelerators in many physics laboratories around the world [2]. The inner part of SRF cavities is made from pure niobium that is in direct contact with a liquid helium bath. The outer shell of the SRF cavities is made from titanium plate which necessitates dissimilar welding of Ti/Nb. Currently the mentioned required dissimilar welding are performed by electron beam in vacuum [1].

Problems in dissimilar welding arise from the differences of physical and chemical properties between the welding counterparts and possible formation of intermetallic brittle phases resulting in the degradation of mechanical properties of welds [3]. However, dissimilar material welding is increasingly demanded from the industry as it can effectively reduce material costs and improve the design [4]. Dissimilar welding using CO_2 continuous lasers has been widely used previously by several researchers around the world [5,6]. Olabi and Co-workers investigated dissimilar laser welding of low carbon steel and AISI316 austenitic steel using CW CO_2 laser [4,5]. They studied full-depth butt welding and costs optimization in this research. During another research, Reisgen et al. studied the CO_2 laser welding of dual phase (DP600) and transformation induced plasticity (TRIP700) steel sheets [6]. Pulsed Nd:YAG laser welding can reduce problems in dissimilar welding due to small heat input, extremely short welding cycle and high accuracy of energy input position [7]. Dissimilar welding of Ti and Fe alloys is one of the most important subjects in this field that has attracted many researchers in the past two decades [8,9]. Since dissimilar welding of Ti and Fe results in brittle intermetallic compounds, interlayer from different metals has been used to achieve an acceptable joint [10,11]. Niobium can be used as interlayer between Ti and Fe because it has no intermetallic compounds with titanium which is the more reactive element chemically [12]. Regarding the binary phase diagram of titanium and niobium (Fig. 1) the particular characteristic of Ti–Nb alloy is the nonappearance of any intermetallic compounds [13]. In order to verify the potential of Nb as a possible candidate for the interlayer between Ti and Fe dissimilar welding, it was considered essential by the research team to study welding behavior of Nb with Ti.

Electron beam welding of Ti–6Al–4V to C-103 (Niobium alloy with 10% Tantalum) for aerospace applications has been reported by Franchini and Pierantozzi [14]. To the best of our knowledge welding of Ti–6Al–4V to Nb using pulsed laser is not reported yet. In pulsed Nd:YAG laser welding of unlike materials, because of high thermal gradients and short thermal cycle, these materials when melted coexist without complete mixing. The above behavior makes pulsed Nd:YAG laser a promising and in comparison with electron beam welding a more economical process for dissimilar materials welding.

In this study butt welding of pure niobium plate to the Ti–6Al–4V titanium alloy sheet using a pulsed Nd:YAG laser is investigated. Effects of various laser and process parameters on the weld profile regarding large difference in thermo-physical properties of

* Corresponding author. Tel.: +98 2182884390.
E-mail address: fmalek@modares.ac.ir (F. Malek Ghaini).

0261-3069/$ - see front matter © 2013 Elsevier Ltd. All rights reserved.
http://dx.doi.org/10.1016/j.matdes.2013.07.094

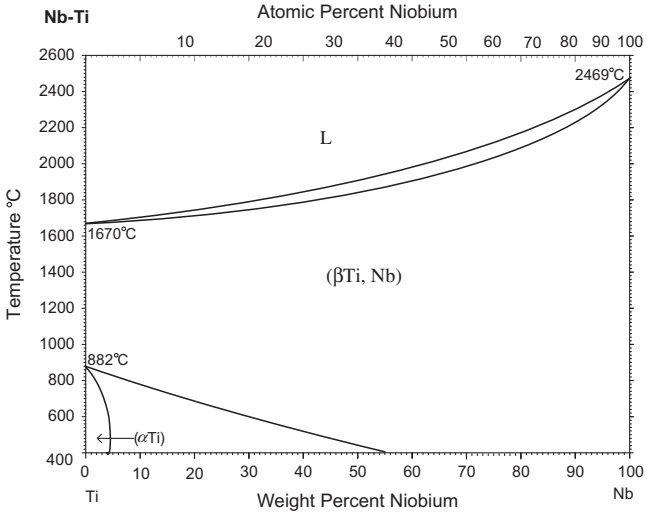

Fig. 1. Binary phase diagram of Ti/Nb [13].

the weld counterparts are studied. The endeavor is directed towards establishing optimum process parameters with regards to the weld metal soundness and the mechanical properties of the joint.

2. Experimental procedures

A pulsed Nd:YAG laser with a maximum mean laser power of 400 W was used. Square shape pulses are the standard output of this laser. The available range for the laser parameters were: 1–1000 Hz for pulse frequency, 0.2–20 ms for pulse duration, and 0–40 J for pulse energy. It is evident that not any arbitrary combination of pulse energy and pulse frequency could be used, as the average laser power could not be more than 400 W. The experiments were conducted with frequencies from 10 to 40 Hz at a constant welding speed of 40 cm/min. The focal length of focusing optical system was 75 mm giving a laser spot size of about 250 μm. For each combination of pulse energy and duration, the laser beam was defocused such that to obtain a constant spot diameter on the work-piece surface. A special fixture was used to hold the sheets of the two materials together, as shown in an earlier article [7]. A translational XYZ controllable table was used to move the fixture with an accurate speed under laser nozzle with 0.05 mm positioning precision.

Pure argon gas with a flow rate of 30 Lit/Min was used as shielding gas commonly on top and bottom of the weld through a particular design. One nozzle, coaxial with the laser beam provides shielding gas on top of the weld line, and another tangential nozzle (a 2 mm inner diameter copper pipe) supplies argon shielding gas for the back side of dissimilar plates around the heated and fusion zones. The materials used for welding were 0.85 mm thick Ti–6Al–4V sheet metal (compatible with AMS 4911H) and 1 mm thick pure niobium (99.9% purity) plates. The plates were cut to 50 mm × 50 mm coupons, cleaned and degreased before the welding process.

To study the weld profile and details of melted zones on both sides of the weld line, the welded samples were sectioned transversely, polished and etched for metallographic examinations. Weld profiles and microstructure were observed by means of optical microscopy and scanning electron microscopy (SEM) equipped with energy dispersive X-ray spectrometry (EDS). Hardness profiles of the weld and base metals were measured using a Vickers micro indentation machine at 200 g load and 10 s. After establishing the optimum process parameters regarding the weld soundness, a number of samples were subjected to mechanical test by an Instron1195 tensile test machine at a cross-head speed of 1 mm/min.

3. Results and discussion

There are many important parameters in pulsed and CW laser welding that have significant effects on the weld profile and should be optimized in each laser welding process [15,16]. The experience gained previously on process parameters and pulsed laser welding of titanium itself, were employed to reduce the number of tests for finding the process window [17]. Thus, some bead on plate welding were conducted on the Ti–6Al–4V sheets to optimize the parameters required for the weld quality and depth of penetration. The results revealed that for the most dominant parameter of pulse peak power (pulse energy divided by the pulse duration), around 1.5 kW is sufficient to achieve full penetration while preventing excessive spatter of the Ti alloy. The next set of experiments concerned the dissimilar joining of Ti–6Al–4V to Nb sheets. Fixing the peak power at 1.5 kW, to investigate the effect of pulse overlapping and duration, a set of experiments were designed as shown in Table 1. It must be emphasized that in the first three experiments the laser beam center was positioned right at the joint line located at the interface of two dissimilar materials while in the last one 70% of laser beam diameter is positioned on Nb and the remained part on the Ti alloy.

Since the welding speed is equal for all samples it would be expected that the average irradiated energy (comparable to the process heat input in conventional welding) will remain constant for the experiments at 27 J/mm. Fig. 2 shows the weld sample TN1 (according to the experiments naming on first column of Table 1). For this experiment the energy packets and their durations are relatively high but their repetition rates and overlapping of the successive pulses [15] are not high.

According to the binary phase diagram of the Ti/Nb (Fig. 1) no inter-metallic compounds will form between these two metals. Moreover, formation of intermetallic compounds between niobium and other alloying elements of Ti–6Al–4V–Al and V-existing in the melt pool is not plausible. Considering the V and Nb binary phase diagram no interaction occurs between niobium and vanadium and for the Al/Nb phase diagram, below 7.5% Al no intermetallic forms [13]. So, obtaining a high-quality dissimilar weld of Ti–6Al–4V/Nb with acceptable mechanical properties can be expected.Generally, in pulsed laser welding by long pulse laser sources, each pulse has its own thermal cycle and creates its

Table 1
Pulsed Nd:YAG Laser welding process parameters for joining Ti–6Al–4V to Nb sheets.

Sample	Pulse energy (J)	Pulse duration (ms)	Welding speed (cm/min)	Pulse repetition rate (Hz)	Overlapping factor (O_f) (%)	Pulse peak power (kw)	Average irradiated energy (J/mm)	Laser beam alignment (%)
TN1	18	12	40	10	38	1.5	27	50–50
TN2	9	6	40	20	68	1.5	27	50–50
TN3	4.5	3	40	40	84	1.5	27	50–50
TN4	4.5	3	40	40	84	1.5	27	70 Nb–30 Ti alloy

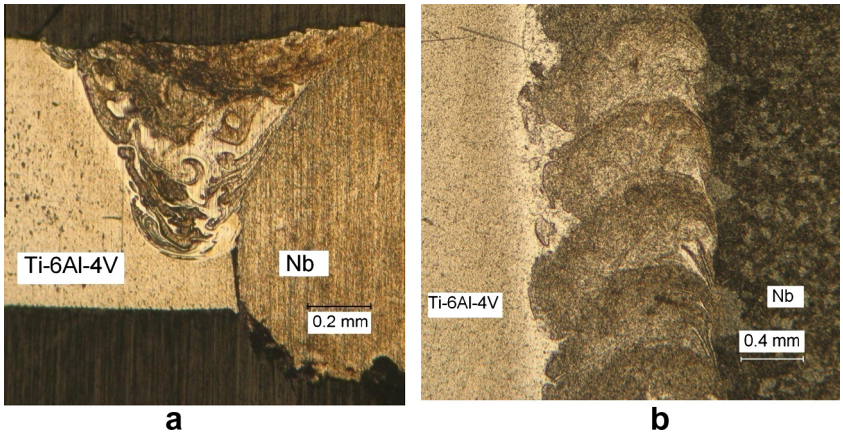

Fig. 2. The TN1 weld sample made at 10 Hz pulse frequency and 18 J pulse energy. (a) Cross section. (b) Top surface as welded.

individual conic weld [18]. A continuous seam weld results from overlapping of individual succeeding pulses (Fig. 3). Description of the overlapping factor was earlier defined and formulated in a previous article [15]. Overlapping factor (O_f) is calculated as:

$$O_f = [1 - (V/f)/(S + VT)] \times 100 \quad (1)$$

where V is the welding speed, f is laser frequency or pulse repetition rate, T is pulse duration and S refers to the laser spot size on work piece that was 1 ± 0.05 mm throughout the tests.

To obtain a complete joint between the weld counterparts a reasonable level of pulse overlapping is required. The overlapping factor calculated for TN1–TN4 samples are shown in Table 1. As seen in Fig. 2a with TN1 condition, it seems that the overlapping factor of 38% would not be enough to achieve sufficient penetration. As shown schematically in Fig. 3, the melting pattern of individual pulses is conic shaped with the greater face crest at the radiation surface. With weld spots just appearing to overlap from the top surface, a continuous penetration through the joint thickness is not obtained.

However, as shown in Fig. 4, with TN2 condition i.e. 20 Hz pulse repetition rate the calculated overlapping factor of successive pulses is increased to 68% and a relatively continuous weld both at the top and bottom of the dissimilar joint is obtained.

With a more careful consideration of Figs. 2 and 4 an interesting observation on the formation of the melt pool can be made. It is seen that that there is a tendency for the melt pool to be pulled irregularly into the Ti–6Al–4V side. According to the binary phase diagram of the Ti/Nb (Fig. 1) it is expected that the melting point of the mixed molten material formed at the interface zone to be between that of Nb and Ti–6Al–4V. Table 2 shows some thermophysical properties of Ti–6Al–4V and niobium [19]. Since the melting point of the Ti–6Al–4V is considerably lower than the mixed melted metal it seems that the melt pool that remains in the liquid state – a little while after laser pulse finish – will propagate in the Ti alloy solid border while the Nb side has been solidified earlier. Furthermore it is possible that due to the lower melting point of the Ti–6Al–4V in comparison with Nb more melting occurs at the Ti side. Similar nonsymmetrical weld pool has been reported by Franchini and Pierantozzi in dissimilar electron beam welding of Ti–6Al–4V and C103 niobium alloy [14].

The SEM image of TN2 sample and the corresponding EDS analysis on three areas in the weld cross section are presented in Fig. 5. It can be seen that although point A is near the Ti side it contains more Nb than Ti and exactly reverse is true for point B which is closer to Nb side. Regularly, it is expected that with penetrating keyhole walls into the metal bulk, the solid phases transform to liquid and the zones near solid borders become richer in elements contained in the nearby solid materials. It seems that in dissimilar pulsed laser welding of Ti–6Al–4V/Nb there are some non-uniform zones like islands that their composition does not obey from the main configuration of the weld metal. As illustrated in weld cross sections of Figs. 2 and 4, brighter zones are mainly composed of Ti while the darker area are richer in Nb element relatively. This means that an intense flow has occurred in the upper part of the pool and Ti and Nb have been thrown to the opposite side of the keyhole. Creation of such fluid flow has been reported by several authors previously [20,21]. Because of temperature and surface tension gradients in the melt pool, Marangoni-driven flow leads to distinct flow patterns during pulsed laser welding.

On the other hand, the composition of point C in Fig. 5 shows the weld metal at the root is indeed significantly richer in Ti. It is known that the laser beam power density decreases by penetrating inside the keyhole depth. Thus, it seems that in the deeper parts of the weld pool the laser intensity is not enough for effective melting of the Nb (with 2468 °C melting temperature) but adequate for melting Ti–6Al–4V.

The above mentioned experiments show with laser beam spot irradiating equally on each part, the weld penetration on Ti alloy will be significantly more than that on the Nb side. TN3 and TN4 weld samples as presented in Table 1 are made with difference only in beam alignment respect to the interface line. Weld TN3 is

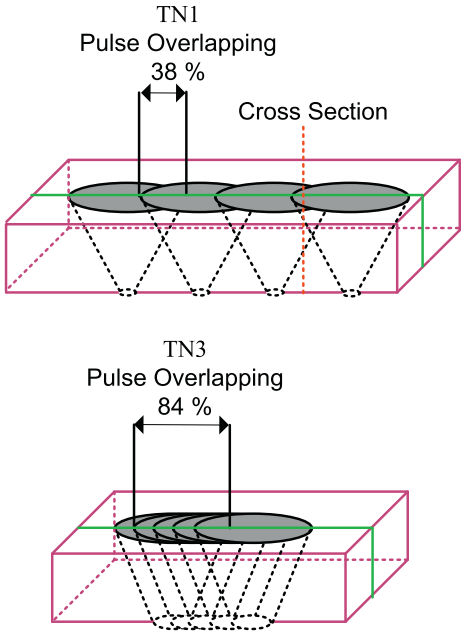

Fig. 3. A schematically drawing to show the overlapping factor definition.

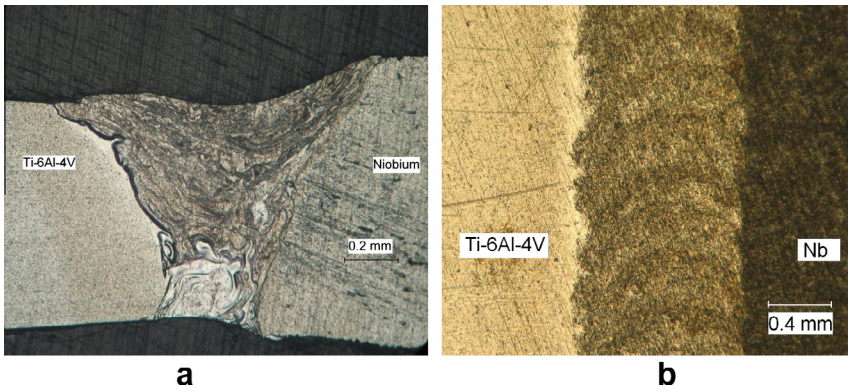

Fig. 4. The TN2 weld sample made at 20 Hz pulse frequency and 9 J pulse energy. (a) Cross section. (b) Top surface as welded.

Table 2
Comparison of thermo-physical properties of Ti–6Al–4V and Niobium [19].

Material	Melting point (°C)	Boiling point (°C)	Density[a] (g/cm^3)	Specific heat[a] C_p (J/(g K))	Thermal conductivity[a] (W/(m K))	Coefficient of linear thermal expansion[a] (m/(m K))
Properties						
Niobium	2468	4900	8.55	0.27	52	7.1×10^{-6}
Ti–6Al–4V	1655	3315	4.43	0.61	6.7	8.6×10^{-6}

[a] Measured at 20 °C.

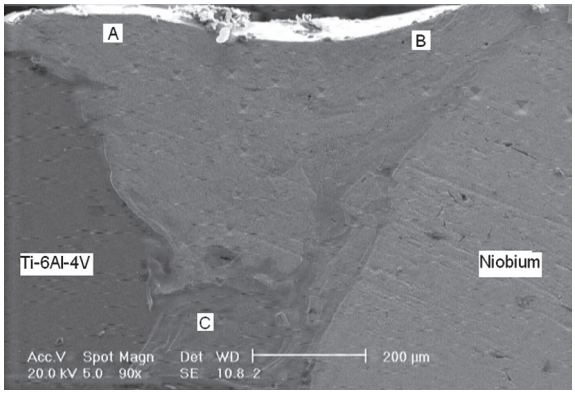

Atomic Percent	Ti	Al	V	Nb
A	41	1	2	56
B	57	3.5	3	36.5
C	75	6	3.5	15.5

Fig. 5. The SEM image and corresponding EDS analysis of the TN2 weld at a cross section in which rich islands of Ti and Nb were identified at the niobium and titanium alloy sides respectively.

made with a 3 ms pulse duration and 4.5 J pulse energy at 40 Hz with 50–50% beam alignment. For weld sample TN4 as schematically shown in Fig. 6, about 70% of the beam diameter was on Nb and only 30% on Ti alloy. Comparing Fig. 7a and b it is observed that the weld pool size for TN3 is significantly larger than that of TN4. Moreover, the weld pool is inclined to the Ti alloy side in TN3 weld. Two reasons for this observation can be proposed.

Because of the higher electrical conductivity of niobium relative to the Ti alloy, the laser absorption in the Nb side of the dissimilar joint is lower. So at the same level of peak power the tendency of weld pool surface evaporation and keyhole formation would be less. It is known that keyhole formation will result in significant increase in the energy absorption by the work piece [15]. Since pulse duration was very short for both TN3 and TN4 samples, there is not enough time for absorption of energy through keyhole on the Nb side. So the energy intake from the laser beam in the Nb side would be less than the Ti alloy side that results in more melting and penetration on the Ti–6Al–4V side.

Regarding Table 2 it can be deduced that thermal conductivity of niobium is more than seven times greater than of the Ti alloy. Moreover the specific heat of the Ti–6Al–4V is about three times greater than niobium. So the energy absorbed in the Nb side dissipates in the bulk and a smaller melting efficiency relative to Ti–6Al–4V would be obtained. In the other words, niobium acts as a sink and Ti alloy as a trap to the energy input current and since the fusion point of Ti–6Al–4V is much lower than Nb (1655 °C relative to 2468 °C) greater melt volume of the Ti alloy is achieved.

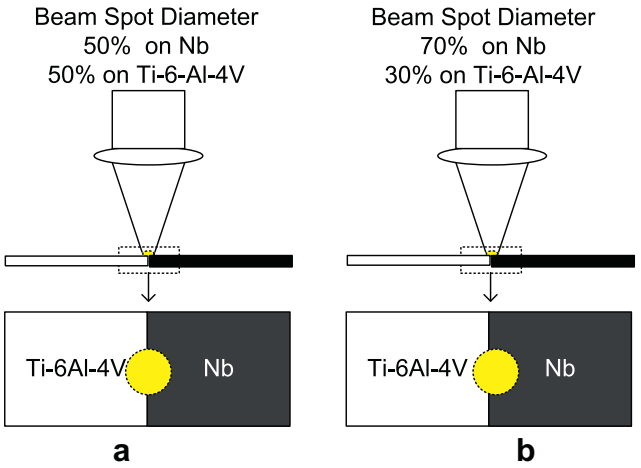

Fig. 6. Schematic drawing of the laser beam alignment (a) TN3 weld with 50% of the beam diameter positioned on each side, and (b) TN4 weld with 70% of the beam positioned on the Nb side.

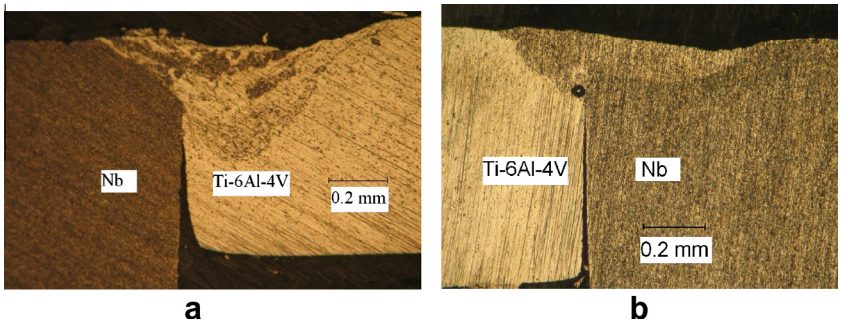

Fig. 7. Cross section of the dissimilar welds between Ti–6Al–4V and Nb sheets with different laser beam alignment. (a) TN3 weld with 50% of the beam positioned on niobium and 50% on Ti alloy and (b) TN4 weld with 70% of the beam positioned on the Nb side.

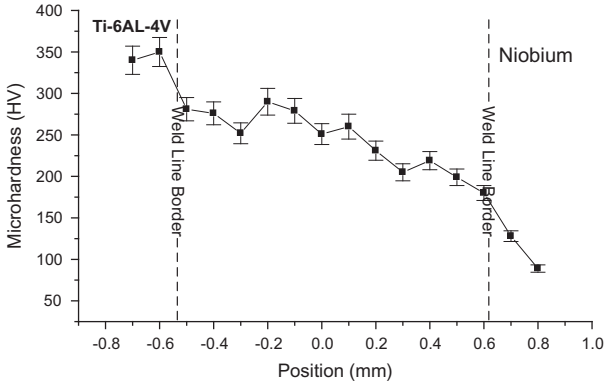

Fig. 8. Micro-hardness profile of the TN2 weld cross section.

Electrical conductivity of Nb/Ti alloy with different titanium weight percent was studied by Read [22] and coworkers found that by increasing Ti contribution the electrical resistivity of the Nb/Ti alloy increases. It means that laser absorption of Nb/Ti alloy surface increases by increasing the titanium weight percent. Going back to the TN1 experiment with 38% overlapping factor, regarding the more absorption of laser energy by the Nb/Ti alloy surface produced in the prior pulses, it can be inferred that the energy intake from laser beam is smaller than that with TN2 at 68% overlapping factor. In the case of TN2 sample the pulse duration and energy are sufficiently high for keyhole formation and its development (compared to the TN3) to attain full penetration among the dissimilar interface of the weld line. As a result, in the TN2 specimen although still low absorption of laser by Nb surface and significant difference in the thermo-physical properties exist but that would not disturb the melting process of dissimilar plate edges and a sound weld is obtained.

Among the above mentioned experiments the best process conditions with regard to weld penetration and soundness i.e. TN2 was selected to evaluate the mechanical properties of Ti–6Al–4V/Nb dissimilar welding. Weld metal hardness was measured using 200 gr load applied for 10 s in the cross section of four specimens welded by the TN2 process parameters. The measurements were performed for the points along a line approximately 0.1 mm below the weld surface in the transverse cross section. The average of the hardness surveys for the four specimens is shown in Fig. 8. The base plate micro-hardness value of the Ti–6Al–4V annealed base plate was 320 ± 20 HV and for Nb sheet it was 80 ± 20 HV. Although the melting point of pure niobium is relatively high, its hardness value as a sheet after forming and annealing processes is very low and it is known as a soft metal [19].

As illustrated in Fig. 8 the maximum hardness value of the dissimilar weld metal is lower than the Ti–6Al–4V base metal. Fluctuations of the hardness value along the pool width can be related to the local composition at each point. The zones containing higher amounts of Ti–6Al–4V are expected to have hardness higher than those regions with higher levels of Nb. However trend of the hardness value along the weld pool width is decreasing from the Ti–6Al–4V to the Nb base metals. The hardness measurement was performed along the depth of the weld and their values were in the range of 220–300 HV except for the brighter region at the bottom of the weld pool of Fig. 4a. The hardness value in this region was relatively higher and reached to 320–350 HV which is close to the hardness of Ti–6Al–4V base metal. This is in confirmation with the results of EDS analysis as presented above (C spot in Fig. 5) and confirms proposition about the development of the keyhole at the Ti–6Al–4V/Nb interface. In the other words the

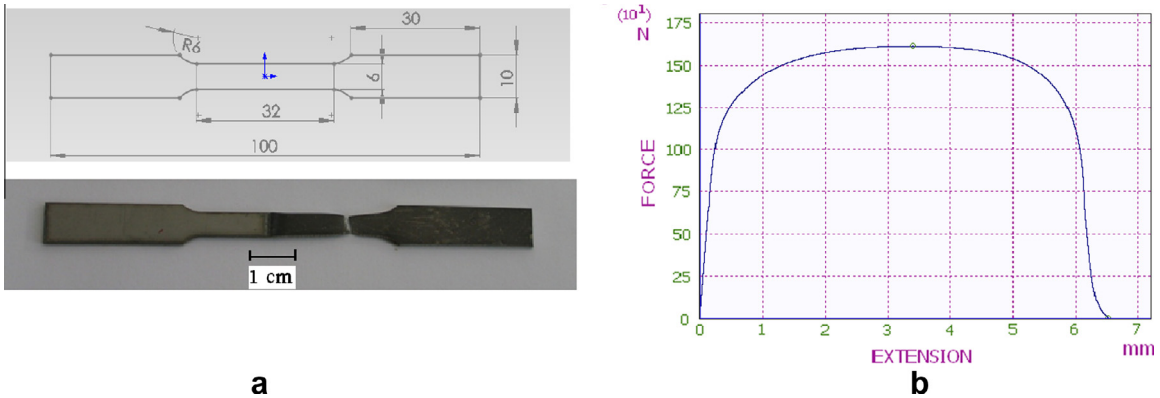

Fig. 9. Tensile test of the TN2 welded with the optimum process parameters; (a) the test sample broken from Nb side and (b) stress/strain curve of dissimilar laser welded Ti–6Al–4V/Nb.

hardness measurement confirms that the weld pool bottom is mainly composed of Ti–6Al–4V.

Tensile testing of the TN2 series dissimilar butt welded specimens was performed to examine the weld strength. The welded sheets were cut by a wire cutting machine to the 100 mm length according to ASTM: E-8M standard. Detailed dimensions of tensile test samples are shown in Fig. 9a.

According to the data provided by the supplier the tensile strength of the annealed Ti–6Al–4V base plate is about 920 MPa which is considerably more than Nb strength. Tensile strength of the annealed technical grade niobium (99.9% purity) is in the range of 250–350 MPa [19]. Impurities, rolling and annealing processes will affect greatly the mechanical properties of niobium plates especially its tensile strength. Myneni and coworkers have studied the mechanical properties of niobium with different levels of purity and produced with various processes [23]. They reported 170–400 MPa for UTS of niobium plates at room temperature.

Four specimens were prepared for the tensile experimentation and were tested. All samples broke on the niobium side and not from the weld metal. As presented in Fig. 9a the Ti–6Al–4V/Nb dissimilar weld was broken from the Nb base metal side. It means that as it was predictable, the weld metal is not brittle, no intermetallic compound could be found and the strength of the joint is more than the softer joint counterpart (niobium base metal). This is in accordance with the Franchini and Pierantozzi results for electron beam welding of Ti–6Al–4V and C103 niobium alloy [14]. As depicted in Fig. 9b, the sample was broken at 162 kN load indicating the Ultimate Tensile Strength (UTS) of the test specimen equal to 269 MPa (Min 254 MPa and Max 277 MPa) which matches the UTS of niobium base plate [19].

4. Conclusions

Dissimilar butt welding of 0.85 mm thick Ti–6Al–4V sheet metal and 1 mm thick pure niobium plates was studied using a pulsed Nd:YAG laser for the first time and regarding weld metal soundness and penetration a set of suitable welding process parameters were established. In summary:

1. As expected from the phase diagram, no intermetallic hard phases were formed in the weld metal. However, small islands of phases rich in Ti and Nb were identified in the fusion zone.
2. It is observed that with more laser energy directed on the Nb side a better mixing and weld profile is obtained particularly at smaller pulse durations such as 3 ms.
3. The laser intensity in the keyhole depth is not enough to melt niobium as effectively as Ti–6Al–4V. So the root of the weld metal is mainly composed of Ti–6Al–4V constituents.
4. At a laser peak power equal to 1.5 kW, among 3, 6 and 12 ms pulse durations, the 6 ms resulted in a full penetration weld.
5. Tensile strength of the full penetration welded joints matched that of the weaker base metal i.e. niobium and the specimens broke outside the fusion zone.

Acknowledgment

The authors would like to thank A. Chehrghani and H. Rahimi for their assistance in the experimental part.

References

[1] Theilacker J, Carter H, Foley M, Hurh P, Klebaner A, Krempetz K, et al. Guidelines for the design, fabrication, testing, installation and operation of SRF cavities. AIP Conf Proc 2009;1218:1223–30.
[2] Cooley LD, Burk D, Cooper C, Dhanaraj N, Foley M, Ford D, et al. Impact of forming, welding, and electropolishing on pitting and the surface finish of SRF cavity niobium. IEEE Trans Appl Supercond 2011;21:2609–14.
[3] Anawa EM, Olabi AG. Control of welding residual stress for dissimilar laser welded materials. J Mater Process Technol 2008;204:22–33.
[4] Olabi AG, Alsinani FO, Alabdulkarim AA, Ruggiero A, Tricarico L, Benyounis KY. Optimizing the CO_2 laser welding process for dissimilar materials. Opt Lasers Eng 2013;51:832–9.
[5] Ruggiero A, Tricarico L, Olabi AG, Benyounis KY. Weld-bead profile and costs optimisation of the CO_2 dissimilar laser welding process of low carbon steel and austenitic steel AISI316. Opt Laser Technol 2011;43:82–90.
[6] Reisgen U, Schleser M, Mokrov O, Ahmed E. Optimization of laser welding of DP/TRIP steel sheets using statistical approach. Opt Laser Technol 2012;44:255–62.
[7] Torkamany MJ, Tahamtan S, Sabbaghzadeh J. Dissimilar welding of carbon steel to 5754 aluminum alloy by Nd:YAG pulsed laser. Mater Des 2010;31:458–65.
[8] Fazel-Najafabadi M, Kashani-Bozorg SF, Zarei-Hanzaki A. Dissimilar lap joining of 304 stainless steel to CP-Ti employing friction stir welding. Mater Des 2011;32:1824–32.
[9] Fuji A, Ameyama K, North TH. Improved mechanical properties in dissimilar Ti-AISI 304L joints. J Mater Sci 1996;31:819–27.
[10] Gao M, Mei SW, Wang ZM, Li XY, Zeng XY. Characterisation of laser welded dissimilar Ti/steel joint using Mg interlayer. Sci Technol Weld Joi 2012;17:269–76.
[11] Tomashchuk I, Sallamand P, Andrzejewski H, Grevey D. The formation of intermetallics in dissimilar Ti6Al4V/copper/AISI 316 L electron beam and Nd:YAG laser joints. Intermetallics 2011;19:1466–73.
[12] Kundu S, Chatterjee S. Evolution of interface microstructure and mechanical properties of titanium/304 stainless steel diffusion bonded joint using Nb interlayer. ISIJ Int 2010;50:1460–5.
[13] ASM handbook volume 03. Alloy phase diagrams. ASM International; 1992. ISBN: 978-0-87170-381-1.
[14] Franchini F, Pierantozzi P. Electron beam welding of dissimilar materials:Niobium-base alloy C-103 with titanium-base alloy Ti–6AI–4V ELI. Weld Int 1992;6:792–9.
[15] Torkamany MJ, Hamedi MJ, Malek F, Sabbaghzadeh J. The effect of process parameters on keyhole welding with a 400 W Nd:YAG pulsed laser. J Phys D Appl Phys 2006;39:4563–7.
[16] Anawa EM, Olabi AG. Using Taguchi method to optimize welding pool of dissimilar laser-welded components. Opt Laser Technol 2008;40:379–88.
[17] Torkamany MJ, Malek Ghaini F, Papan E, Dadras S. Process optimization in titanium welding with pulsed Nd:YAG laser. Sci Adv Mater 2012;4:489–96.
[18] Sabbaghzadeh J, Azizi M, Torkamany MJ. Numerical and experimental investigation of seam welding with a pulsed laser. Opt Laser Technol 2008;40:289–96.
[19] Grill R, Gnadenberger A. Niobium as mint metal: production–properties–processing. Int J Refract Metal Hard Mater 2006;24:275–82.
[20] Pitscheneder W, DebRoy T, Mundra K, Ebner R. Role of sulfur and processing variables on the temporal evolution of weld pool geometry during multikilowatt laser beam welding of steels. Weld J 1996;75:71.
[21] Zhao X, Kwakernaak C, Pan Y, Richardson IM, Saldi Z, Kenjeres S, et al. The effect of oxygen on transitional Marangoni flow in laser spot welding. Acta Mater 2010;58:6345–57.
[22] Read DT. Metallurgical effects in niobium-titanium alloys. Cryogenics 1978;18:579–84.
[23] Myneni GR, Umezawa H. Variation of mechanical properties of high RRR and reactor grade niobium with heat treatments. Mater Tech 2003;7–9:19–22.